The Dynamics of a Single Algebraic Screw Pair

J.D. Robinson[1], M.J.D. Hayes[2]
[1] *Department of Mechanical and Aerospace Engineering, Carleton University, jrobins7@connect.carleton.ca*

[2] *Department of Mechanical and Aerospace Engineering, Carleton University, jhayes@mae.carleton.ca*

Abstract
The algebraic screw pair, or A-pair, represents a new class of kinematic constraint that exploits the self-motions inherent to a specific configuration of Griffis-Duffy platform. Using the A-pair as a joint in a hybrid parallel-serial kinematic chain results in a sinusoidal coupling of rotation and translation between adjacent links. The resulting linkage is termed an A-chain. This paper reveals the dynamic equations of motion of a single A-pair and examines the impact of the inertial properties of the legs of the A-pair on the dynamics. A numerical example illustrates the impact of the leg effects from different perspectives and shows that while the gravity effects of the legs is significant it may be possible to neglect the leg kinetic energy from the dynamics model.

Keywords: Algebraic screw pair, Griffis-Duffy platform, dynamic equations of motion.

Dynamique d'une paire algébrique de vis

Résumé
La paire algébrique de vis, ou l'A-paire, représente une nouvelle classe de la contrainte cinématique qui exploite les individu-mouvements inhérents à une configuration spécifique de plateforme de Griffis-Duffy. Utilisant les A-paires comme joint dans résultats à chaînes cinématiques parallèle-périodiques hybrides d'un accouplement sinusoïdal de rotation et de traduction entre adjacent liens. La tringlerie en résultant se nomme une A-chaîne. Ce document indique les équations du mouvement dynamiques d'une seule A-paire et examine l'impact des propriétés à inertie des jambes des A-paires sur la dynamique. Un exemple numérique illustre l'impact des effets de jambe de différentes perspectives et montre cela tandis que les effets de pesanteur des jambes est significatif il peuvent être possibles pour négliger l'énergie cinétique de jambe du modèle de dynamique.

Mots-clé: Paire algébrique de vis, plateforme de Griffis-Duffy, équations du mouvement dynamiques.

1 INTRODUCTION

The algebraic screw pair [1], or A-pair, is a novel kinematic pair based on a specific configuration of parallel manipulator called the Griffis-Duffy platform (GDP) [2]. The GDP is a special configuration of the six legged, six degree-of-freedom (DOF) Stewart-Gough platform (SGP) that, in most configurations, is subject to self-motions regardless of the state of the actuated legs. Self-motions are situations where the end effector (EE) of the manipulator can move in an uncontrolled manner without actuator input. The rationale behind proposing the A-pair is based on the hypothesis that replacing the revolute pairs (R-pairs) in a serial manipulator with this special configuration of parallel platform will enhance the rigidity of the serial arm. At the time of this writing an actuated prototype 4A-chain, shown in Figure 1 a), is being constructed that will be used to investigate the rigidity hypothesis. The focus of this paper is the examination of the dynamics of a single A-pair including an examination of the effects of the inertial properties of the legs of the GDP. A numerical example based on the joints of the prototype manipulator is presented to illustrate the magnitude of the leg effects in a real application.

2 THE ALGEBRAIC SCREW PAIR

In 1993 Griffis and Duffy [2] introduced the GDP, a special configuration of the SGP characterized by a planar fixed base and planar moving platform each with six specially placed spherical joint anchor points for the six legs of the manipulator. The anchor points lie on the perimeter of a triangle on each of the fixed base and moving platform. Six of the anchor points are located one on each of the vertices of the two triangles and the remaining six anchor points are located one on each edge of the triangles such that each leg has one anchor point on the fixed base and one anchor point on the moving platform. Figure 1 b) shows one example of a GDP, many other configurations

a) 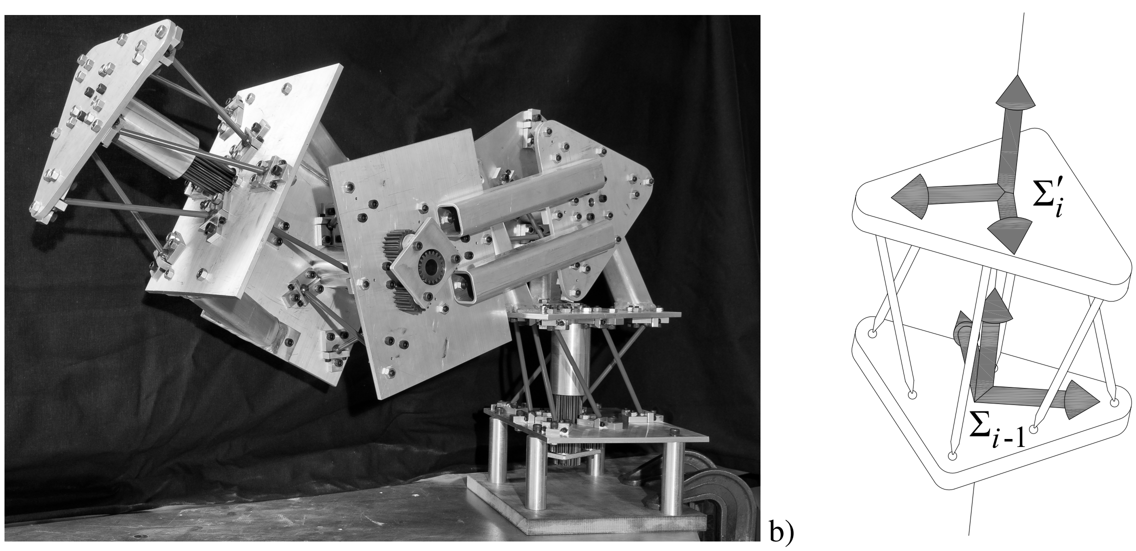 b)

Figure 1: a) Prototype 4A-chain currently being constructed. b) Example of a GDP. The configuration shown is the midline-to-vertex configuration.

exist. Griffis and Duffy proposed controlling the end effector, EE, of the manipulator (affixed to the moving platform) by controlling the length of each of the six legs. With this definition of a GDP there are many possible configurations, however the work presented here focuses on one particular configuration called the midline-to-vertex configuration, illustrated in Figure 1 b), where a leg with an anchor point at one of the vertices of the fixed base has an anchor point on the midpoint of one of the edges of the triangle on the moving platform and vice versa, maintaining the same order of legs around the perimeter of the fixed base and moving platform.

A significant issue with GDPs is self-motions. Self-motions represent instances where a manipulator can move in an uncontrolled manner without actuator input. For a GDP this means that the moving platform moves relative to the fixed base without changing the length of the legs. Husty and Karger address the self-motions of SGPs in general in [3, 4] and focus on GDPs in [5], showing that most configurations of GDP, including the midline-to-vertex, are always subject to self-motions regardless of the lengths of the actuated legs throughout the entire reachable workspace volume. Normally the existence of self-motions, especially throughout the entire reachable workspace, is an undesirable characteristic thus the GDP is widely considered to be a failure as a parallel manipulator. An interesting characteristic of the midline-to-vertex GDP self-motions is that they possess one well-defined, uncontrollable degree-of-freedom (DOF) [5].

For the remainder of this paper a special GDP configuration is used that possesses the following constraints: the fixed base and moving platform anchor point triangles are congruent equilateral triangles with each side of the triangles being of length a and the six legs are all of a fixed length, l, equal to the height, h, of the triangles as illustrated in Figure 2a). The value of l is

$$l = h = \frac{a\sqrt{3}}{2}. \tag{1}$$

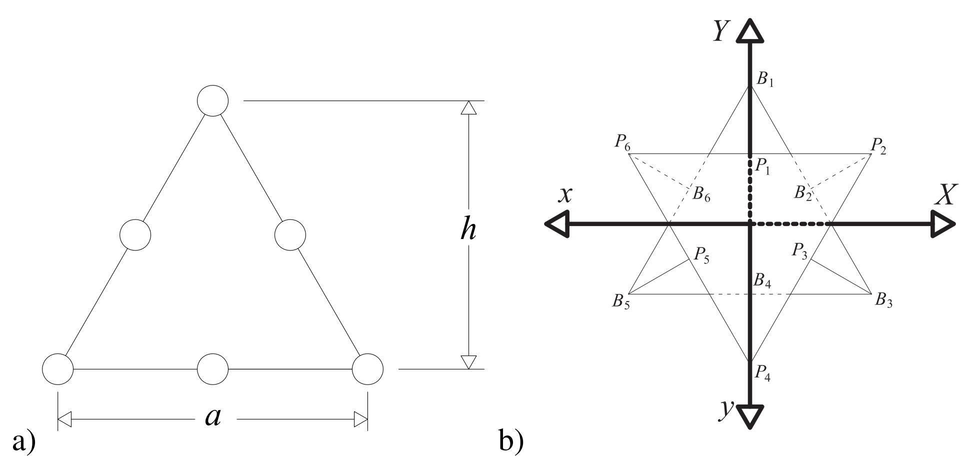

Figure 2: a) The height, h, of the congruent equilateral fixed base and moving platform triangles is equal to the distance from the midpoint of one side of the triangle to the opposite vertex. The sides of the triangles are of length a. b) Coordinate systems and positions of leg anchor points on the fixed base and moving platform when $\theta = 180°$. The $\hat{z}$ axes of both frames point out of the page.

It turns out that the self-motions of this GDP couple rotation about an axis passing through the geometric centres of both the fixed base and moving platform triangles with translation along that axis. Husty and Karger [5] show that the separation of the fixed base and moving platform, d, is a function of the rotation angle, θ, about the axis common to both the fixed base and moving platform:

$$d = \rho \sin\left(\frac{\theta}{2}\right), \tag{2}$$

where ρ is a function of the geometry of the GDP. When $\theta = 0°$ the GDP is said to be in its *home position*. This is a theoretical reference position that can only be achieved if collisions between the physical elements that constitute the GDP are ignored because in the home position $d = 0$ and the fixed base and moving platform are coincident. When the platform is fully extended, similar to Figure 1 b), $\theta = 180°$ and $d = \rho$. This fully extended position and the geometry of the GDP are used to determine the value of the constant ρ as

$$d(\theta = 180°) = \rho = \frac{a\sqrt{6}}{3}. \tag{3}$$

It is proposed in [6] to utilize the well-defined one DOF self-motion of this special GDP as a joint in a serial chain in place of standard R-pairs. The motivation behind this is that beyond the rotation and translation about and along the joint axis the truss-like structure of the parallel platform makes it very rigid in all other directions. This new type of joint, or kinematic pair, is called and algebraic screw pair because it couples translation and rotation like a screw pair with the exception that the pitch of the screw can be represented as an algebraic function of the rotation angle (tangent of the half-angle substitution is used to represent the trigonometric function as an algebraic function). The direct kinematics and inverse kinematics of A-chains are explored in [1, 6] and the workspaces of short A-chains are examined in [7].

The remainder of this paper describes how the dynamic equations of motion are obtained for a single A-pair using the Lagrange formulation both with the assumption that the leg inertia effects are negligible and with the legs considered as slender rods. The results are compared to determine the validity of the massless leg assumption.

3 DYNAMICS

This section discusses the general derivation of the dynamic model using the Lagrangian formulation [8, 9] and applies the technique to the single A-pair first without and then with leg inertia.

3.1 Lagrange Formulation of the Dynamics

The Lagrangian formulation of the dynamic equations of motion utilizes generalized coordinates, q_i, $i = 1, \ldots, n$, to describe the pose of an n degree-of-freedom serial manipulator independent of the reference frames. The Lagrangian of the system is defined as $\mathcal{L} = \mathcal{T} - \mathcal{U}$, where $\mathcal{T}$ is the total kinetic energy of the system and $\mathcal{U}$ is the total potential energy of the system. The Lagrangian equations can be written in a compact form as

$$\frac{d}{dt}\left(\frac{\partial \mathcal{L}}{\partial \dot{\mathbf{q}}}\right)^T - \left(\frac{\partial \mathcal{L}}{\partial \mathbf{q}}\right)^T = \boldsymbol{\xi}, \tag{4}$$

where $\mathbf{q}$ is the vector of the joint variables and $\boldsymbol{\xi}$ is a vector of the non conservative generalized forces, such as the joint actuator torques and joint torques induced by friction and the forces and moments applied to the EE. In order to use the Lagrangian equations one must first determine the total kinetic and potential energy of the system.

3.1.1 Kinetic Energy

The total kinetic energy in a serial chain is given by $\mathcal{T} = \sum_{i=1}^{n}(\mathcal{T}_{\ell_i})$, where $\mathcal{T}_{\ell_i}$ is the kinetic energy of Link i. The kinetic energy of Link i is given by

$$\mathcal{T}_{\ell_i} = \frac{1}{2} m_{\ell_i} \dot{\mathbf{p}}_{\ell_i}^T \dot{\mathbf{p}}_{\ell_i} + \frac{1}{2} \boldsymbol{\omega}_i^T \mathbf{R}_i \mathbf{I}_{\ell_i}^i \mathbf{R}_i^T \boldsymbol{\omega}_i, \tag{5}$$

where m_{ℓ_i} is the mass of Link i, $\dot{\mathbf{p}}_{\ell_i}$ is the linear velocity of the link's centre of gravity (CG) ($\mathbf{p}_{\ell_i}$ is the position of the CG), $\boldsymbol{\omega}_i$ is the angular velocity of the link, $\mathbf{R}_i$ is the rotation matrix from the reference frame for Link i to the base frame, and $\mathbf{I}_{\ell_i}^i$ is the link's moment of inertia tensor with respect to the Link i reference frame. The linear and angular velocities of Link i can be written as $\dot{\mathbf{p}}_{\ell_i} = \mathbf{J}_P^{(\ell_i)} \dot{\mathbf{q}}$, and $\boldsymbol{\omega}_i = \mathbf{J}_O^{(\ell_i)} \dot{\mathbf{q}}$, where the $\mathbf{J}_P^{(\ell_i)}$ and $\mathbf{J}_O^{(\ell_i)}$ Jacobian matrices are assembled by accounting for only the joint motion between the Link i and the base, *i.e.* the $3 \times n$ matrices

$$\mathbf{J}_P^{(\ell_i)} = \begin{bmatrix} \boldsymbol{\jmath}_{P_1}^{(\ell_i)} & \cdots & \boldsymbol{\jmath}_{P_i}^{(\ell_i)} & 0 & \cdots & 0 \end{bmatrix}, \quad \mathbf{J}_O^{(\ell_i)} = \begin{bmatrix} \boldsymbol{\jmath}_{O_1}^{(\ell_i)} & \cdots & \boldsymbol{\jmath}_{O_i}^{(\ell_i)} & 0 & \cdots & 0 \end{bmatrix}, \tag{6}$$

where for a prismatic joint $\boldsymbol{\jmath}_{P_j}^{(\ell_i)} = \hat{z}_{j-1}$ and $\boldsymbol{\jmath}_{O_j}^{(\ell_i)} = \mathbf{0}$ and for an R-pair $\boldsymbol{\jmath}_{P_j}^{(\ell_i)} = \hat{z}_{j-1} \times (\mathbf{p}_i - \mathbf{p}_{j-1})$ and $\boldsymbol{\jmath}_{O_j}^{(\ell_i)} = \hat{z}_{j-1}$. The total kinetic energy of the manipulator is written as

$$\mathcal{T} = \textstyle\sum_{i=1}^{n} (\mathcal{T}_{\ell_i}) = \frac{1}{2} \dot{\mathbf{q}}^T \mathbf{B}(\mathbf{q}) \dot{\mathbf{q}}, \quad \mathbf{B}(\mathbf{q}) = \sum_{i=1}^{n} \left(m_{\ell_i} \mathbf{J}_P^{(\ell_i)T} \mathbf{J}_P^{(\ell_i)} + \mathbf{J}_O^{(\ell_i)T} \mathbf{R}_i \mathbf{I}_{\ell_i}^i \mathbf{R}_i^T \mathbf{J}_O^{(\ell_i)} \right). \tag{7}$$

$\mathbf{B}(\mathbf{q})$ is the $n \times n$ inertial matrix.

3.1.2 Potential Energy

The total potential energy of the system with non-flexible members is written as

$$\mathcal{U} = -\sum_{i=1}^{n} \left(m_{l_i} \mathbf{g}_0^T \mathbf{p}_{l_i} \right), \tag{8}$$

where $\mathbf{g}_0$ is the gravity acceleration vector in the base frame ($\mathbf{g}_0 = \begin{bmatrix} 0 & 0 & -g \end{bmatrix}^T$).

3.1.3 Equations of Motion

The Lagrangian equations are now written as

$$\mathbf{B}(\mathbf{q})\ddot{\mathbf{q}} + \mathbf{n}(\mathbf{q}, \dot{\mathbf{q}}) = \boldsymbol{\xi}, \quad \text{where} \quad \mathbf{n}(\mathbf{q}, \dot{\mathbf{q}}) = \dot{\mathbf{B}}(\mathbf{q})\dot{\mathbf{q}} - \tfrac{1}{2} \left(\tfrac{\partial}{\partial \mathbf{q}} (\dot{\mathbf{q}}^T \mathbf{B}(\mathbf{q}) \dot{\mathbf{q}}) \right)^T + \left(\tfrac{\partial \mathcal{U}(\mathbf{q})}{\partial \mathbf{q}} \right)^T. \tag{9}$$

The joint space dynamic model can be written as

$$\mathbf{B}(\mathbf{q})\ddot{\mathbf{q}} + \mathbf{C}(\mathbf{q}, \dot{\mathbf{q}})\dot{\mathbf{q}} + \mathbf{F}_v \dot{\mathbf{q}} + \mathbf{F}_s \mathrm{sgn}(\dot{\mathbf{q}}) + \mathbf{g}(\mathbf{q}) = \boldsymbol{\tau} - \mathbf{J}^T(\mathbf{q})\mathbf{h}_e, \tag{10}$$

where $\mathbf{h}_e$ is the vector of forces and moments exerted by the EE on the environment, $\mathbf{J}^T(\mathbf{q})\mathbf{h}_e$ gives the portion of the actuator torques used to exert that force, $\mathbf{F}_s$ is the $n \times n$ diagonal matrix representing the static friction coefficients, $\mathbf{F}_s\mathrm{sgn}(\dot{\mathbf{q}})$ is a simplified model of the static friction and depends on the direction of the joint velocities, $\mathbf{F}_v$ is the $n \times n$ diagonal matrix of viscous friction coefficients, $\mathbf{g}(\mathbf{q})$ is the final term of the equation for $\mathbf{n}(\mathbf{q}, \dot{\mathbf{q}})$ where

$$g_i(\boldsymbol{\theta}) = \frac{\partial \mathcal{U}}{\partial \theta_i} = -\sum_{j=1}^{n} \left(m_{\ell_j} \mathbf{g}_0^T \boldsymbol{J}_{P_i}^{(\ell_j)}(\boldsymbol{\theta}) \right), \tag{11}$$

and the elements of the $n \times n$ matrix $\mathbf{C}(\mathbf{q}, \dot{\mathbf{q}})$ are found by

$$c_{ij} = \sum_{k=1}^{n} c_{ijk}\dot{q}_k, \quad c_{ijk} = \frac{1}{2}\left(\frac{\partial b_{ij}}{\partial q_k} + \frac{\partial b_{ik}}{\partial q_j} + \frac{\partial b_{jk}}{\partial q_i} \right), \tag{12}$$

where c_{ijk} are Christoffel symbols of the first type [8] and $\mathbf{C}(\mathbf{q}, \dot{\mathbf{q}})$ contains the Coriolis and centrifugal terms [8].

3.2 Dynamics of a Single A-Pair Ignoring Leg Inertia

When the inertial properties of the legs are assumed negligible the mass of the legs may be ignored completely or included in the mass of the moving platform. A reference coordinate systems is affixed to the fixed base, Σ_0, and moving platform, Σ_1. The Σ_0 origin is located at the geometric centre of the fixed base triangle, the $\hat{z}_0$ axis points along the A-pair axis of rotation towards the moving platform and the $\hat{x}_0$ and $\hat{y}_0$ axes are arbitrarily assigned in the plane of the fixed base anchor point triangle. Σ_1 is established such that Σ_0 and Σ_1 are coincident when the A-pair is in the home position. Σ_1 moves with the moving platform as the A-pair is actuated. Figure 2b) shows how the coordinate systems are affixed to the A-pair and the positions of the leg anchor points. For this paper the CG of the moving link is considered to be located at the origin of Σ_1. The Lagrange formulation with $n = 1$ is used to obtain the dynamic equations of motion.

With $n = 1$ the linear component of the link Jacobian is $\mathbf{J}_P^{(link)} = \frac{\partial \mathbf{p}_{link}}{\partial \theta} = \begin{bmatrix} 0 & 0 & \frac{a\sqrt{6}}{6}\cos\left(\frac{\theta}{2}\right) \end{bmatrix}^T$ and the angular component of the link Jacobian is $\mathbf{J}_O^{(link)} = \begin{bmatrix} 0 & 0 & 1 \end{bmatrix}^T$. The $\mathbf{B}(\theta)$ matrix is found using Equation (7) as

$$\mathbf{B}(\theta) = m_{link}\mathbf{J}_P^{(link)T}\mathbf{J}_P^{(link)} + \mathbf{J}_O^{(link)T}\mathbf{R}_1\mathbf{I}_{link}^1\mathbf{R}_1^T\mathbf{J}_O^{(link)} = \frac{a^2 m_{link}}{6}\cos^2\left(\frac{\theta}{2}\right) + I_{zz}, \tag{13}$$

where I_{zz} is mass moment of inertia of the moving platform about the z_1 axis. Using the trigonometric identity

$$\cos^2\left(\frac{\theta}{2}\right) = \frac{1 + \cos(\theta)}{2} \tag{14}$$

The $\mathbf{B}(\theta)$ and $\mathbf{C}(\theta, \dot{\theta})$ terms become

$$\mathbf{B}(\theta) = \tfrac{a^2 m_{link}}{12}\left(1 + \cos(\theta)\right) + I_{zz}, \quad \mathbf{C}(\theta, \dot{\theta}) = \tfrac{1}{2}\left(\tfrac{\partial \mathbf{B}(\theta)}{\partial \theta}\right)\dot{\theta} = \tfrac{a^2 m_{link}}{24}\sin(\theta)\,\dot{\theta}. \tag{15}$$

The gravitational (potential energy) term is obtained by Equation (11) as

$$g_i(\boldsymbol{\theta}) = -m_{link}\mathbf{g}_0^T\mathbf{J}_P^{link} = \frac{a m_{link} g\sqrt{6}}{6}\cos\left(\frac{\theta}{2}\right). \tag{16}$$

Assembling the dynamic equations in the joint space using Equation (10) gives

$$\tau_1 = \left(\frac{a^2 m_{link}}{12}\left(1+\cos(\theta)\right) + I_{zz}\right)\ddot{\theta} + \frac{a^2 m_{link}}{12}\sin(\theta)\,\dot{\theta}^2 + \frac{a m_{link} g\sqrt{6}}{6}\cos\left(\frac{\theta}{2}\right). \tag{17}$$

Equation (17) provides the solution to the inverse dynamics problem which allows for the determination of the joint torque profile required to follow a provided trajectory ($\theta(t)$, $\dot{\theta}(t)$ and $\ddot{\theta}(t)$ profiles), ignoring friction and external forces. If the torque and joint state are specified Equation (17) can be rearranged to solve for the acceleration, $\ddot{\theta}$, yielding the solution to the direct dynamics problem.

3.3 Dynamics of a Single A-Pair Considering Leg Inertias

The Lagrange formulation is well suited to modelling the leg effects into the dynamic equations for A-pairs because the leg influences are found by determining the kinetic and potential energy of each leg (which are functions of θ) and including them in the Lagrangian. The symmetry of the A-pair means that the kinetic energy effects of only one leg needs to be examined and then multiplied by six to account for all legs. The potential energy of each individual leg depends on the orientation of the A-pair. For a vertical joint (gravity vector parallel to joint axis) all legs have the same potential energy, in other orientations the potential energy is determined using the combined CG of the six legs (a point on the joint axis equidistant from the fixed base and moving platform).

3.3.1 Kinetic Energy of the Legs

The kinetic energy of the leg has two components: the linear motion of the leg CG and the angular motion about the leg anchor point on the fixed base. The leg is modelled as a slender rod and thus the kinetic energy from any rotation about the centre axis of the leg is considered to be negligible.

Figure 2b) shows that the position vector of the fixed base anchor point of Leg 1, B_1, in Σ_0 is $\mathbf{b}_1 = \begin{bmatrix} 0 & \frac{a\sqrt{3}}{3} & 0 \end{bmatrix}^T$ and the position of the moving platform anchor point for Leg 1, P_1, in Σ_1 is ${}^1\mathbf{p}_1 = \begin{bmatrix} 0 & -\frac{a\sqrt{3}}{6} & 0 \end{bmatrix}^T$. A point on the moving platform projects onto a circle in the $\hat{x}_0$-$\hat{y}_0$ plane as θ varies, while the $\hat{z}_0$ position is given by Equation (2). The position vector of P_1 in Σ_0 is $\mathbf{p}_1 = \begin{bmatrix} \frac{a\sqrt{3}}{6}\sin\theta & -\frac{a\sqrt{3}}{6}\cos\theta & \frac{a\sqrt{6}}{3}\sin\left(\frac{\theta}{2}\right) \end{bmatrix}^T$. The vector along the leg from B_1 to P_1 is

$$\mathbf{r}_{P_1/B_1} = \mathbf{p}_1 - \mathbf{b}_1 = \begin{bmatrix} \frac{a\sqrt{3}}{6}\sin\theta & -\frac{a\sqrt{3}}{6}(2+\cos\theta) & \frac{a\sqrt{6}}{3}\sin\left(\frac{\theta}{2}\right) \end{bmatrix}^T, \tag{18}$$

and the position vector of the CG of Leg 1 is

$$\mathbf{p}_{leg} = \mathbf{b}_1 + \frac{1}{2}\mathbf{r}_{P_1/B_1} = \begin{bmatrix} \frac{a\sqrt{3}}{12}\sin\theta & \frac{a\sqrt{3}}{12}(2-\cos\theta) & \frac{a\sqrt{6}}{6}\sin\left(\frac{\theta}{2}\right) \end{bmatrix}^T. \tag{19}$$

The linear velocity component Jacobian for the CG of the leg comes from $\frac{\partial \mathbf{p}_{leg}}{\partial \theta}$ and is

$$\mathbf{J}_P^{(leg)}(\theta) = \left[\begin{array}{ccc} \frac{a\sqrt{3}}{12}\cos\theta & \frac{a\sqrt{3}}{12}\sin\theta & \frac{a\sqrt{6}}{12}\cos\left(\frac{\theta}{2}\right) \end{array} \right]^T, \tag{20}$$

and the linear velocity of the leg CG is $\dot{\mathbf{p}}_{leg} = \mathbf{J}_P^{(leg)}(\theta)\dot{\theta}$. The linear component of the kinetic energy of Leg 1 with mass M_{leg}, utilizing Equation (14), is

$$T_{P_{leg}} = \frac{1}{2} m_{leg} \dot{\mathbf{p}}_{leg}^T \dot{\mathbf{p}}_{leg} = \frac{1}{2} m_{leg} \mathbf{J}_P^{(leg)T} \mathbf{J}_P^{(leg)} \dot{\theta}^2 = \frac{a^2 m_{leg}}{96} \left(2 + \cos\left(\theta\right)\right) \dot{\theta}^2. \tag{21}$$

The angular component of the kinetic energy requires the determination of the angular velocity of the leg. The velocity of P_1 with respect to B_1, $\mathbf{v}_{P_1/B_1} = \dot{\mathbf{r}}_{P_1/B_1}$ is the time rate of change of $\mathbf{r}_{P_1/B_1}$ where the only variable that is a function of time is θ. Therefore

$$\mathbf{v}_{P_1/B_1} = \left[\begin{array}{ccc} \frac{a\sqrt{3}}{6}\cos\theta & \frac{a\sqrt{3}}{6}\sin\theta & \frac{a\sqrt{6}}{6}\cos\left(\frac{\theta}{2}\right) \end{array} \right]^T \dot{\theta}. \tag{22}$$

A reference coordinate system for the leg is established with its origin at B_1 such that $\hat{z}_{leg}$ points along the leg from B_1 towards P_1, $\hat{y}_{leg}$ is parallel to $\mathbf{v}_{P_1/B_1}$ and $\hat{x}_{leg}$ completes the right hand system. Since the leg is represented as a slender rod the and there is no rotation about $\hat{y}_{leg}$ (it is parallel to the velocity vector), only the magnitude of the leg angular velocity of the leg about $\hat{x}_{leg}$, $\omega_{x_{leg}}$, is of concern. It is obtained by dividing the velocity of P_1 with respect to B_1 by the distance from B_1 to P_1, which gives

$$\omega_{x_{leg}} = \frac{||\mathbf{v}_{P_1/B_1}||}{||\mathbf{r}_{P_1/B_1}||} = \frac{1}{3}\sqrt{2 + cos\left(\theta\right)}\dot{\theta}. \tag{23}$$

The inertia tensor for the slender rod representing the leg in the leg reference frame is

$$\mathbf{I}_{leg}^{(leg)} = \left[\begin{array}{ccc} \frac{a\sqrt{3}}{6} m_{L_1} & 0 & 0 \\ 0 & \frac{a\sqrt{3}}{6} m_{L_1} & 0 \\ 0 & 0 & 0 \end{array} \right], \tag{24}$$

where the length of the leg is given in Equation (1). The angular kinetic energy of Leg 1 is

$$T_{O_{leg}} = \frac{1}{2}\omega_{x_{leg}}^2 I_{xx_{leg}} = \frac{\sqrt{3}}{108} a m_{leg} \left(2 + \cos\left(\theta\right)\right) \dot{\theta}^2. \tag{25}$$

The summation of Equation (21) and Equation(25) represents the total kinetic energy of each A-pair leg. The total kinetic energy of all of the legs is six times this value.

3.3.2 Potential Energy of the Legs

The potential energy of Leg 1 from Equation (8) is $\mathcal{U}_{leg} = m_{leg}\mathbf{g}_0^T \mathbf{p}_{leg}$, and the gravity term of the dynamic equations from Equation (11) is

$$g_{leg} = \frac{\partial \mathcal{U}}{\partial \theta} = -m_{leg}\mathbf{g}_0^T \mathbf{J}_P^{(leg)} = \frac{m_{leg} g a \sqrt{6}}{12} \cos\left(\frac{\theta}{2}\right). \tag{26}$$

Equation (26) assumes that g_0 is parallel to the joint axis. In situations where the A-pair is not vertical the component of gravity vector that is parallel to the joint axis is used.

3.3.3 Influence of Legs On the Dynamic Equations

The impact of all of the legs on the dynamic equations of motion is found by multiplying each leg term by six. The inertial term for the six legs, $\mathbf{B}_{legs}(\theta)$, is obtained from Equation (21) and Equation (25) and the $\mathbf{C}_{legs}(\dot{\theta}, \theta)$ term comes from Equation (12) to give

$$\mathbf{B}_{legs}(\theta) = \tfrac{am_{leg}}{144}\left(9a + 8\sqrt{3}\right)(2 + \cos(\theta)), \quad \mathbf{C}_{legs}(\dot{\theta}, \theta) = \tfrac{am_{leg}}{288}\left(9a + 8\sqrt{3}\right)\sin(\theta)\,\dot{\theta}. \tag{27}$$

The gravitational term for all six legs, $\mathbf{g}_{legs}(\theta)$, is six times Equation (26):

$$\mathbf{g}_{legs}(\theta) = \frac{m_{leg} g a \sqrt{6}}{2} \cos\left(\frac{\theta}{2}\right). \tag{28}$$

The dynamic equations of motion of the A-pair with the mass effects of the legs included is

$$\tau = \left(\mathbf{B}_{link}(\theta) + \mathbf{B}_{legs}(\theta)\right)\ddot{\theta} + \left(\mathbf{C}_{link}(\dot{\theta}, \theta) + \mathbf{C}_{legs}(\dot{\theta}, \theta)\right)\dot{\theta} + \left(\mathbf{g}_{link}(\theta) + \mathbf{g}_{legs}(\theta)\right). \tag{29}$$

In general the leg masses are much smaller than the link masses and the $\mathbf{B}_{legs}(\theta)$ and $\mathbf{C}_{legs}(\dot{\theta}, \theta)$ terms have a much larger denominator than the corresponding terms for the link, therefore the potential energy term for the legs has a larger impact than the kinetic energy terms, however the overall influence depends on the ratio of the link mass to the mass of the legs (see Section 5 for a numerical example). When the difference between the masses is small the leg effects will be more pronounced and should be included and when the difference is large it may be possible to ignore the leg effects. The choice to include or exclude leg effects depends on the application and desired dynamic model fidelity. When additional terms are introduced such as motor inertias, friction and external applied loads the impact of the leg effects on model fidelity will be further diminished.

4 Numerical Example

The impact of the inclusion of leg effects on the dynamics of a single A-pair are best illustrated by a numerical example. The mass properties for this example are derived from the first joint in the prototype serial A-chain shown in Figure 1 a) being constructed by the authors of this paper. The mass of the single link, m_{link}, is the mass of the A-pair moving platform and the various components attached to it. The moving platform is approximated as an 10 *in* by 8 *in* plate weighing 4.135 *lb* and the CG of the plate lies on the joint axis. The moment of inertia about the joint axis is $I_{zz} = \frac{m_{l_1}}{12}(10^2 + 8^2)$. Each of the six legs is a 6 *in* long slender rod weighing 0.115 *lb*. The length of the sides of the fixed base and moving platform triangles are found by rearranging Equation (1) to get $a = 6.928$ *in*. The acceleration due to gravity is $g = 386.4$ *in/s*^{s}.

The A-pair is examined in two orientations, the first vertical, where the joint axis is parallel to the gravity vector and the potential energy terms dominate the dynamic equations and the second horizontal, where the joint axis is perpendicular to the gravity vector and the kinetic energy terms dominate. Friction is not included in this analysis. All simulations were run using MATLAB Simulink software. The assigned joint trajectory ($\theta(t)$, $\dot{\theta}(t)$ and $\ddot{\theta}(t)$) rotated the A-pair from a stationary $\theta = 60°$ to a stationary $\theta = 300°$ in ten seconds. The different dynamic models are compared using the total work done to follow the assigned trajectory.

In the vertical orientation the effects of gravity on the A-pair motion are most evident. The four different versions of the dynamic model compared are: massless legs, leg mass included as part of the link (lumped mass), leg effects fully accounted for (with legs), and considering only the leg potential energy terms (PE only). Equation (29) is used to obtain the dynamic equations and determine the torque required to follow the given trajectory. The appropriate mass values and the resulting total torque required to follow the desired trajectory are provided in Table 1. The torque time histories of the various models following the desired trajectory are provided in Figure 3a).

Table 1: Masses and total work done for the different dynamic models of the single A-pair in the vertical and horizontal orientations.

			Total Work	
Model	$m_{link}g$	$m_{leg}g$	Vertical	Horizontal
Massless Legs	4.135 *lb*	0 *lb*	28.52 *in-lb*	0.0897 *in-lb*
Lumped Mass	4.825 *lb*	0 *lb*	33.28 *in-lb*	0.1047 *in-lb*
With Legs	4.135 *lb*	0.115 *lb*	30.89 *in-lb*	0.0916 *in-lb*
PE Only	4.135 *lb*	0.115 *lb*	30.89 *in-lb*	N/A

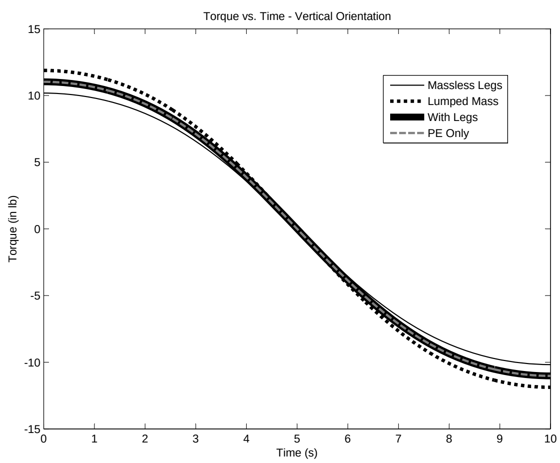

(a) Vertical orientation.

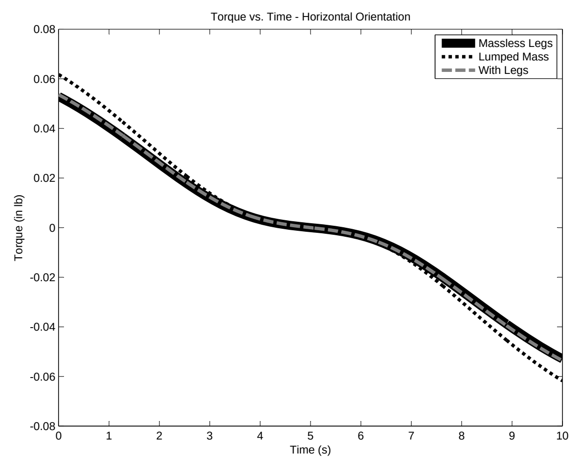

(b) Horizontal orientation.

Figure 3: Torque vs. time plots for the various models of an A-pair.

When the A-pair axis is horizontal the gravity effects are removed and, since friction is ignored, the inertial effects of the link and legs dominate the dynamic equations. Three versions of the dynamic model, massless legs, lumped mass, and with legs are compared in Table 1. The torque time histories of the various models following the desired trajectory are provided in Figure 3b).

4.1 Discussion

The two different orientations of the A-pair considered illustrate the impact of the inertial effects of the legs on the potential energy terms (vertical) and kinetic energy terms (horizontal). Analysis of the results provides some insight as to how to account for the leg effects in longer chains. The decision as to include leg effects or not and which model to use depends on the desired fidelity and the relative masses of the links and legs.

When the A-pair axis is vertical the potential energy effects of the link and legs dominate the dynamic equations (with friction ignored) and the kinetic energy effects are essentially negligible. For the masses used in the numerical example the total work done for the massless legs model is 6% less than that of the full leg model which is in turn 7% less than the lumped mass model. If the difference between the link and leg mass is increased these percent differences decrease. For example if the link mass increases to 8 *lb* there is a 4% difference in total work done between the full leg and lumped mass models. While the reason for the underestimation of the magnitude of the required torque by the massless legs model is obvious (the leg mass has been completely ignored) the difference between the lumped mass and full leg models results from the difference in the change in potential energy of the link versus the leg. As the trajectory is followed the difference in height of the link CG from the minimum to the maximum is 2.829 *in* while the CG of the legs varies by only 1.414 *in*. In the lumped mass model the change of potential energy for the leg mass is twice the actual value. The combined potential energy of the six legs can be determined by a point mass equal to the total mass of the six legs on the joint axis equidistant to the fixed base and moving platform planes. Using this CG model allows for the determination of the leg potential energy when the A-pair joint axis is tilted away from vertical.

In the horizontal orientation the potential energy terms go to zero and only the kinetic energy terms are evident. The lumped mass model overestimates the total work by 14% while the massless leg model underestimates the total work by only 2%. This suggests that for the masses used in this example the kinetic energy effects of the legs may be considered to be negligible.

The results of this numerical example suggests that little fidelity is lost if the leg kinetic energy terms are ignored, however the leg potential energy terms are important.

5 Conclusions and Future Considerations

This paper presents the derivation of the dynamic equations using the Lagrange formulation for a single A-pair with and without the mass effects of the A-pair legs. The development of the equations is presented in such a way that similar techniques could be used to obtain the dynamic equations for longer chains constructed using A-pairs or any other simple kinematic pair. The inclusion of the leg mass effects into the dynamic equations is explored theoretically and via a numerical example. The gravitational effects of the combined six legs have a larger impact on the overall dynamic model relative to the inertial effects. The decision to include the leg effects depends on the desired model fidelity and the relative difference in mass between the link and legs. As the ratio of link mass to leg mass increases the impact of the legs on the dynamics decreases. In the numerical example it is reasonable to ignore the inertial leg effects, however the inclusion of the gravitational effects of the legs is important. This paper explores the dynamics of a single A-pair and future work will extend to chains with more joints. There are some aspects of the single A-pair dynamics that must be examined in more detail. This paper has ignored friction, motor, and transmission effects in the dynamic analysis. Motors and transmissions will add mass to the links, further diminishing the the effects of legs on the overall dynamics. The work presented in this paper is a starting point for the process of sizing and selecting motors. Also, the inclusion of a friction model will further diminish the percentage of torque required to overcome the leg mass effects, thereby further decreasing the impact of the legs on the dynamic model.

REFERENCES

[1] J.D. Robinson and M.J.D. Hayes. The kinematics of a-pair jointed serial linkages. In *Proceedings of The ASME International Design and Techncal Conferences, IDETC 2010*, Montreal, Quebec, Canada, August 2010.

[2] M.W. Griffis and J. Duffy. Method and apparatus for controlling geometrically simple parallel mechanisms with distinctive connections. U.S. Patent Number: 5,179,525, 1993.

[3] A. Karger and M.L. Husty. Classification of all self-motions of the original Stewart-Gough platform. *Computer-Aided Design*, 30(3):205–215, 2007.

[4] M.L. Husty and A. Karger. Self motions of Stewart-Gough platforms, an overview. In *Proceedings of the workshop on fundamental issues and future research directions for parallel mechanisms and manipulators*, pages 131–141, Quebec City, Canada, October 2002.

[5] M.L. Husty and A. Karger. Self-motions of Griffis-Duffy type parallel manipulators. In *Proceedings of ICRA '00 IEEE International Conference on Robotics and Automation*, pages 7–12, San Francisco, CA, USA, April 2000.

[6] J.D. Robinson. Direct and inverse kinematics of a new class of parallel-serial hybrid manipulator. Master's thesis, Carleton University, Canada, 2008.

[7] J.D. Robinson and M.J.D. Hayes. Reachable workspace comparison of revolute pair jointed and algebraic screw pair jointed kinematic chains. In *Proceedings of The Canadian Society for Mechanical Engineering Forum 2010*, Victoria, British Columbia, Canada, June 2010.

[8] B. Siciliano, L. Sciavicco, L. Villani, and G. Oriolo. *Robotics Modelling, Planning and Control*. Springer-Verlag London Limited, London, 1995.

[9] L. Sciavicco and B. Siciliano. *Modeling and Control of Robot Manipulators*. McGraw-Hill, Inc., New York, 1996.